

Maximized Orbital and Spin Kondo effects in a single-electron transistor

Karyn Le Hur¹, Pascal Simon², and László Borda^{3,4}

¹ *Département de Physique and RQMP, Université de Sherbrooke, Sherbrooke, Québec, Canada, J1K 2R1*

² *Laboratoire de Physique et Modélisation des Milieux Condensés et
Laboratoire d'Etude des Propriétés Electroniques des Solides, CNRS
25 av. des martyrs, 38042 Grenoble, France*

³ *Sektion Physik and Center for Nanoscience, LMU München, 80333 München, Theresienstr. 37 and*

⁴ *Research Group of the Hungarian Academy of Sciences, Institute of Physics, TU Budapest, H-1521*

(Dated: October 29, 2018)

We investigate the charge fluctuations of a single-electron box (metallic grain) coupled to a lead via a smaller quantum dot in the Kondo regime. The most interesting aspect of this problem resides in the interplay between *spin* Kondo physics stemming from the screening of the spin of the small dot and *orbital* Kondo physics emerging when charging states of the grain with (charge) $Q = 0$ and $Q = e$ are almost degenerate. Combining Wilson's numerical renormalization-group method with perturbative scaling approaches we push forward our previous work [K. Le Hur and P. Simon, Phys. Rev. B 67, 201308R (2003)]. We emphasize that for symmetric and slightly asymmetric barriers, the strong entanglement of charge and spin flip events in this setup inevitably results in a non trivial stable SU(4) Kondo fixed point near the degeneracy points of the grain. By analogy with a small dot sandwiched between two leads, the ground state is Fermi-liquid like which considerably smears out the Coulomb staircase behavior and hampers the Matveev logarithmic singularity to arise. Most notably, the associated Kondo temperature $T_K^{SU(4)}$ might be raised compared to that in the conductance experiments through a small quantum dot ($\sim 1K$) which makes the observation of our predictions *a priori* accessible. We discuss the robustness of the SU(4) correlated state against the inclusion of an external magnetic field, a deviation from the degeneracy points, particle-hole symmetry in the small dot, asymmetric tunnel junctions and comment on the different crossovers.

PACS numbers: 75.20.Hr, 71.27.+a, 73.23.Hk

I. INTRODUCTION

Recently, quantum dots have attracted a considerable interest due to their potential applicability as single electron transistors or as basic building blocks (qubits) in the fabrication of quantum computers.¹ In the last years, a great amount of work has also been devoted to studying the Kondo effect in mesoscopic structures.² A motivation for these efforts was the recent experimental observation of the Kondo effect in tunneling through a small quantum dot in the Kondo regime.^{3,4,5} In these experiments, the excess electronic *spin* of the dot acts as a magnetic impurity. Let us also mention that the manipulation of magnetic cobalt atoms on a copper surface and more specifically the observation of the associated Kondo resonance via spectroscopy tunneling measurements^{6,7} also stands for a remarkable opportunity to probe spin Kondo physics at the mesoscopic scale but in another realm (not with artificial structures).

A different set of problems relating the Kondo effect to the physics of quantum dots is encountered when investigating the charge fluctuations of a large Coulomb-blockaded quantum dot (metallic grain).⁸ More precisely, one of the most important features of a quantum dot is the Coulomb blockade phenomenon, i.e., as a result of the strong repulsion between electrons, the charge of a quantum dot is quantized in units of the elementary charge e . Even a metallic dot at a micronmetric scale can still behave as a good single-electron transistor. When the gate voltage V_g is increased the charge

of the grain changes in a step-like manner. This behavior is referred to as a Coulomb staircase. Moreover when the metallic dot is weakly-coupled to a bulk lead, so that electrons can hop from the lead to the dot and back, the dot charge remains to a large extent quantized. This quantization has been investigated with thoroughness both theoretically^{9,10,11,12} and experimentally.¹³ It is important to bear in mind that such a problem is intrinsically connected to an *orbital* or charge Kondo effect.⁹ Indeed, near the degeneracy points of the average charge in the grain one can effectively map the problem of charge fluctuations onto a (planar) two-channel Kondo Hamiltonian^{14,15,16} with the two charge configurations in the box playing the role of the impurity spin^{9,17} and the physical spin of the conduction electrons acting as a passive channel index. (This mapping is *a priori* valid only for weak tunneling junctions between the grain and the lead). For accessible temperatures – in general, larger than the level spacing of the grain – spin Kondo physics is not relevant.¹⁸ The quantity of interest is the average dot charge as a function of the voltage applied to a back-gate. Note that the average dot charge can be measured with sensitivity well below a single charge.¹⁹ Unfortunately, only some fingerprints of the two-channel Kondo effect were recently observed for a setting in semiconductor quantum dots.²⁰ Indeed, the non-Fermi liquid nature of the two-channel Kondo effect is hardly accessible in the Matveev's setup built on semiconducting devices.²¹ On the one hand, the charging energy of the grain must be large enough to maximize the Kondo temperature

T_K on the other hand the level spacing must be small enough compared to T_K . It is difficult to satisfy these two conflicting limits. A better chance for observing the two-channel Kondo behavior may be reached if tunneling between the lead and the grain involves a resonant level since it offers the possibility to actually enhance the Kondo temperature of the system.²²

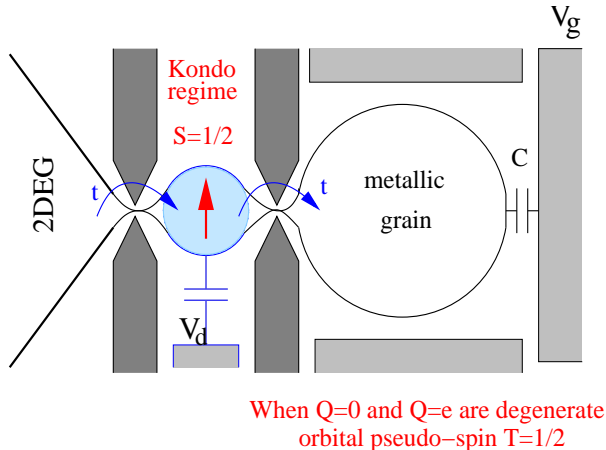


FIG. 1: Schematic view of the setup. A micron scale grain (or large dot) is weakly coupled to a bulk lead via a small dot in the Kondo regime which acts as an $S=1/2$ spin impurity. The charges of the grain and the small dot are controlled by the gate voltage V_g and V_d respectively. The auxiliary voltages can be used to adjust the tunnel junctions.

In this paper, the setup we analyze consists of a single-electron box or grain coupled to a reservoir through a smaller dot (Figure 1). We assume that the smaller dot contains an odd number of electrons and eventually acts as an $S=1/2$ Kondo impurity.² Typically, when only charge Kondo flips are involved the low energy physics near the degeneracy points is well described by a two-channel Kondo model, in particular the capacitance peaks of the grain exhibit at zero temperature a logarithmic singularity at the degeneracy points which ensures a nice Coulomb staircase even for not too weak couplings between the quantum box and the lead.⁹ In our setup, the Kondo effect has now two possible origins: the spin due to the presence of the small dot playing the role of an $S=1/2$ spin impurity and the orbital degeneracy on the grain. Combining Wilson's numerical renormalization-group (NRG) method with perturbative scaling approaches we extend our previous work,²³ and emphasize that at (and near) the degeneracy points of the grain, the two Kondo effects can be intertwined. The orbital degrees of freedom of the grain become strongly entangled with the spin degrees of freedom of the small dot resulting in a stable fixed point with an $SU(4)$ symmetry. This requires symmetric or slightly asymmetric tunneling junctions. Furthermore, the low energy fixed point is a Fermi-liquid which considerably smears out the Coulomb staircase behavior and hampers the Matveev logarithmic singularity to arise.⁹ Remember that the ma-

major consequence of this enlarged symmetry in our setup is that the grain capacitance exhibits instead of a logarithmic singularity, a strongly reduced peak as a function of the back-gate voltage, smearing charging effects in the grain considerably. It is also worth noting that the Kondo effect is maximized when both Kondo effects occur simultaneously. In particular, the associated Kondo temperature $T_K^{SU(4)}$ can be strongly enhanced compared to that of the Matveev's original setup which may guarantee the verification of our predictions. We stress that the Coulomb staircase behavior becomes smeared out already in the weak tunneling limit due to the appearance of spin-flip assisted tunneling. A different limit where the small dot rather acts as a resonant level close to the Fermi level has been studied in Refs. [22,24] where in contrast it was shown that the resonant level has only a slight influence on the smearing of the Coulomb blockade even if the transmission coefficient through the impurity is one at resonance. This differs markedly from the case of an energy-independent transmission coefficient where the Coulomb staircase is completely destroyed for perfect transmission.^{9,25} Furthermore, the charge of the grain in such a device can be used to measure the occupation of the dot.²⁴ The resonant-level behavior of Ref. [24] is also recovered in our setup when an orbital magnetic field is applied.

Let us mention that the possibility of a strongly correlated Kondo ground state possessing an $SU(4)$ symmetry has also been discussed very recently in the different context of two small dots coupled with a strong capacitive inter-dot coupling.²⁶ The possibility of orbital and spin Kondo effects in such a geometry was previously anticipated by Schön *et al.*²⁷ inspired by preliminary experiments of Ref. [28]. It is worth noting that these types of problems have also potential connections with the twofold orbitally degenerate Anderson impurity model^{30,31} and more precisely with the physics of certain heavy fermions like UBe_{13} where the U ion is modeled by a non-magnetic quadrupolar doublet²⁹ and then quadrupolar (orbital) and spin Kondo effects can in principle interfere.³⁰

Our paper is structured as follows: In Section II, we resort to a Schrieffer-Wolff transformation and derive the effective model including the different useful parameters. In Section III, assuming that we are far from the degeneracy points of the grain we use a pedestrian perturbation theory; This reveals the importance of spin flips even in this limit. In Section IV, we carefully investigate both theoretically and numerically the interplay between orbital and spin Kondo effects at the degeneracy points. In Section V, we discuss in details the effects of possible symmetry breaking perturbations and the crossovers generated by such perturbations. Finally, section VI is devoted to the discussion of our results and especially we summarize our main experimental predictions for such a setup.

II. MODEL AND SCHRIEFER-WOLFF TRANSFORMATION

In the sequel, we analyze in details the behavior of charge fluctuations in the grain. In order to model the setup depicted in Figure 1, we consider the Anderson-like Hamiltonian:

$$\begin{aligned}
 H = & \sum_k \epsilon_k a_{k\sigma}^\dagger a_{k\sigma} + \sum_p \epsilon_p a_{p\sigma}^\dagger a_{p\sigma} + \frac{\hat{Q}^2}{2C} + \varphi \hat{Q} \\
 & + \sum_\sigma \epsilon a_\sigma^\dagger a_\sigma + U n_\uparrow n_\downarrow \\
 & + t \sum_{k\sigma} \left(a_{k\sigma}^\dagger a_\sigma + h.c. \right) + t \sum_{p\sigma} \left(a_{p\sigma}^\dagger a_\sigma + h.c. \right),
 \end{aligned} \tag{1}$$

where $a_{k\sigma}$, a_σ , $a_{p\sigma}$ are the annihilation operators for electrons of spin σ in the lead, the small dot, and the grain, respectively, and t is the tunneling matrix element which we assume to be k independent for simplification. Let us first consider that tunnel junctions are *symmetric*. We also assume that junctions are narrow enough and contain one transverse channel only. Extensions of the model to asymmetric or larger junctions will be analyzed later in section V. We also assume that the energy spectrum in the grain is continuous, which implies that the grain is large enough such that its level spacing Δ_g is very small compared to its charging energy $E_c = e^2/(2C)$: $\Delta_g/E_c \rightarrow 0$ (in Ref. [20] $\Delta_g \sim 70\text{mK}$ was not sufficiently small compared to the Kondo temperature scale which hindered the logarithmic capacitance peak⁹ to completely develop). \hat{Q} denotes the charge operator of the grain, C is the capacitance between the grain and the gate electrode, and φ is related to the back-gate voltage V_g through $\varphi = -V_g$. $\epsilon < 0$ and U are respectively the energy level and charging energy of the small dot, and $n_\sigma = a_\sigma^\dagger a_\sigma$. The inter-dot capacitive coupling is assumed to be weak and therefore neglected.

We mainly focus on the particularly interesting situation where the small dot is in the *Kondo regime*, which requires the last level to be singly occupied and the condition

$$t \ll -\epsilon, U + \epsilon, \tag{2}$$

to be satisfied ($\epsilon < 0$). The resonant level limit where ϵ lies near the Fermi level will be addressed at some points in Section V. In the local moment regime, we can integrate out charge fluctuations in the small dot using a generalized Schrieffer-Wolff transformation.^{32,33} More precisely, the system is described by the Hamiltonian:

$$\begin{aligned}
 H = & \sum_k \epsilon_k a_k^\dagger a_k + \sum_p \epsilon_p a_p^\dagger a_p + \frac{\hat{Q}^2}{2C} + \varphi \hat{Q} \\
 & + \sum_{m,n} \left(\frac{J}{2} \vec{S} \cdot \vec{\sigma} + V \right) a_m^\dagger a_n.
 \end{aligned} \tag{3}$$

To simplify the notations, the spin indices have been omitted and hereafter. m, n take values in the two sets

“lead” (k) or “grain” (p), the spin \vec{S} is the spin of the small dot, $\vec{\sigma}$ are Pauli matrices acting on the spin space of the electrons. Let us now discuss the parameters J and V in more details.

In the vicinity of one degeneracy point obtained for $\varphi = -e/2C$, where the grain charging states with $Q = 0$ and $Q = e$ are degenerate, we find explicitly:

$$J = 2t^2 \left[\frac{1}{-\epsilon} + \frac{1}{U + \epsilon} \right]. \tag{4}$$

A small direct hopping term

$$V = \frac{t^2}{2} \left[\frac{1}{-\epsilon} - \frac{1}{U + \epsilon} \right], \tag{5}$$

is also present and should not be neglected. In particular, this embodies the so-called “charge flips” from the reservoir to the grain and vice-versa in the Matveev’s original problem. Notice that the ratio V/J can take values between $-1/4$ (when $U = -\epsilon$) and $1/4$ (when $U \rightarrow \infty$). $V = 0$ corresponds to the particle-hole symmetric case where $2\epsilon + U = 0$. For $\varphi = -e/2C$, the energy to add a hole or an electron onto the metallic grain vanishes and therefore the Schrieffer-Wolff parameters V and J are completely identical to those of a small dot connected to two metallic reservoirs.³⁴ Furthermore, remember that in the present model the ultraviolet cutoff at which the effective model becomes valid can be roughly identified to $D \sim \min\{E_c, \Delta_d\}$ where Δ_d is the level spacing of the small dot (with today’s technology it is possible to reach⁵ $\Delta_d \sim 2\text{-}3\text{K}$ and for the grain²⁰ $E_c \sim 2.3\text{K}$).

On the other hand, far from the degeneracy point $\varphi = -e/2C$ – which means on a charge plateau – the energy to add a *hole* on the grain is $U_{-1} = E_c(1 + 2N)$ where $N = CV_g/e \neq 1/2$. Similarly, it costs $U_1 = E_c(1 - 2N)$ to add an extra *electron* onto the grain. The lead-dot and grain-dot Kondo couplings, J_0 and J_1 respectively, then become *asymmetric* even for symmetric junctions:

$$J_0 = 2t^2 \left[\frac{1}{-\epsilon} + \frac{1}{U + \epsilon} \right] = J \tag{6}$$

$$J_1 = 2t^2 \left[\frac{1}{U_1 - \epsilon} + \frac{1}{U + \epsilon + U_{-1}} \right].$$

In the second equation, the virtual intermediate state where an electron first hops from the grain onto the small dot induces an excess of energy U_{-1} in the second term. The first term contains the energy of the intermediate state of the process where the temporal order of the hopping events is reversed. The off-diagonal terms where an electron from the reservoir [grain] flips the impurity spin and then jumps onto the grain [reservoir] reads

$$J_{01} = 2t^2 \left[\frac{1}{U_1 - \epsilon} + \frac{1}{U + \epsilon} \right] \tag{7}$$

$$J_{10} = 2t^2 \left[\frac{1}{-\epsilon} + \frac{1}{U + \epsilon + U_{-1}} \right].$$

Note that in general particle-hole symmetry is absent in the large dot, so in principle $J_{01} \neq J_{10}$. But, in our setting, $E_c = e^2/2C \ll |\epsilon|, U + \epsilon$, so in the following we will neglect the asymmetry between J_{01} and J_{10} far from the degeneracy points ($J_{01} = J_{10}$) (this has no drastic consequence on the results). In the finite temperature range $T < U_1, U_{-1}$, these off-diagonal processes are suppressed exponentially as $\tilde{J}_{10} = J_{10}(T) \approx J_{10}e^{-U_1/4kT}$, whereas the diagonal spin processes can be strongly renormalized at low temperatures. In other words, in the Renormalization Group language, if we start at high temperature with a set of Kondo couplings J_0, J_1, J_{01}, J_{10} , the growing of J_{01}, J_{10} is cut-off when T is decreased below $\max(U_1, U_{-1})$ whereas the growing of J_0, J_1 is not. This offers a room to reach a 2-channel Kondo effect in the spin sector (for asymmetric tunneling junctions) provided the condition $J_0 = J_1$ can be reached with a fine-tuning of the gate voltages.³⁵ We can do the same approximation for the V term and define V_{10}, V_{01} accordingly (with $V_{10} = V_{01}$) and also \tilde{V}_{10} .

III. PEDESTRIAN PERTURBATION THEORY ON A PLATEAU

We want first to compute the corrections to the average charge on the grain on a charge plateau due to the Kondo and V couplings bearing in mind that when the tunneling amplitude $t \rightarrow 0$, the average grain charge $\langle \hat{Q} \rangle$ exhibits perfect Coulomb staircase behavior as a function of V_g . We confine ourselves to values of φ in the range $-e/(2C) < \varphi < e/(2C)$, which corresponds to the unperturbed (charge) value $Q = 0$. A first natural approach is to assume that the Kondo and charge-flip couplings are very small compared to the charging energy $E_c = e^2/(2C)$ of the grain and to calculate the corrections to $Q = 0$ in perturbation theory. Despite this perturbative calculation will appear of limited use, it is very instructive to perform it in order to point the different sources of divergences that appear when approaching the degeneracy points, the main issue treated in this paper. At second order, we find

$$\langle \hat{Q} \rangle_2 = e \left(\frac{3}{8} J_{10}^2 + 2V_{10}^2 \right) \ln \left(\frac{e/2C - \varphi}{e/2C + \varphi} \right). \quad (8)$$

Note that at finite low temperature $T < U_1, U_{-1}$, we should use the renormalized off-diagonal couplings $\tilde{J}_{10}, \tilde{V}_{10}$ which are small (in other words the flow of the off-diagonal Kondo couplings has been cut-off for $T < U_1, U_{-1}$). This better reproduces the (exact) numerical calculations of Ref. 12. For more details, we refer the reader to Appendix A. The density of states in the lead and in the grain have been assumed to be equal⁹ and taken to be 1 for simplicity. This result tends to trivially generalize that of a grain directly coupled to a lead.⁹ However, there are two reasons that may suggest this perturbative approach is divergent. Higher-order terms – already at cubic order – involve logarithmic divergences as-

sociated to the renormalizations of the Kondo couplings (see Appendix A), but also other logarithms indicating the vicinity of the degeneracy point $\varphi = -e/2C$ in the charge sector. For example, a correction at cubic order to the result in Eq. (8) is given by

$$\langle \hat{Q} \rangle_3 \propto J_0 J_{10}^2 \ln \left(\frac{D}{k_B T} \right) \ln \left(\frac{e/2C - \varphi}{e/2C + \varphi} \right), \quad (9)$$

We also have a similar correction in $J_1 J_{10}^2$. It would be potentially interesting to observe the logarithmic temperature-dependence of $\langle \hat{Q} \rangle$ on a given plateau due to Kondo spin-flip events. Note also that the perturbation theory in the V_{10} term has been previously extended to the fourth order.¹⁰ The perturbative result is valid only far from the degeneracy points provided the renormalization, e.g., of the spin Kondo coupling J_0 is also cut-off either by the temperature T or by a magnetic field B [in general, for symmetric junctions one already gets $J_0 > J_1$ at the bare level; See Eq. (6)]. This considerably restricts the range of application of this perturbative calculation compared for example to the simpler setup involving a grain coupled to a reservoir and even on a charge plateau the temperature must be larger than the emerging spin Kondo energy scale between the lead and the small dot. Finally, note that in our perturbative treatment at finite temperature $T < U_1, U_{-1}$ we have made the (standard) approximation: We have only virtually introduced the temperature through the renormalization of the couplings J_{10} and V_{10} .

The other regimes which requires non-perturbative approaches will be studied in Sections IV and V.

IV. ORBITAL AND SPIN KONDO EFFECTS CLOSE TO THE DEGENERACY POINTS

In this section, we will be primarily interested in the situation close to the degeneracy point $\varphi = -e/2C$ where none of the perturbative arguments above can be applied. We want to show that the Hamiltonian given by Eq. (3) can be mapped onto some generalized Kondo Hamiltonian following Ref. [9].

A. Mapping to a generalized Kondo model

Close to the degeneracy point $\varphi = -e/2C$ and for $k_B T \ll E_c$, only the states with $Q = 0$ and $Q = e$ are accessible and higher energy states can be removed from our theory introducing the projectors \hat{P}_0 and \hat{P}_1 (which project on the states with $Q = 0$ and $Q = e$ in the grain respectively). The truncated Hamiltonian (3) then reads:

$$H = \sum_{k, \tau=0,1} \epsilon_k a_{k\tau}^\dagger a_{k\tau} \left(\hat{P}_0 + \hat{P}_1 \right) + eh\hat{P}_1 \quad (10)$$

$$+ \sum_{k, k'} \left[\left(\frac{J}{2} \vec{\sigma} \cdot \vec{S} + V \right) \left(a_{k1}^\dagger a_{k'0} \hat{P}_0 + a_{k'0}^\dagger a_{k1} \hat{P}_1 \right) \right]$$

$$+ \sum_{\tau=0,1} \left(\frac{J}{2} \vec{\sigma} \cdot \vec{S} + V \right) a_{k\tau}^\dagger a_{k'\tau} \Big],$$

where now the index $\tau = 0$ indicates the reservoir and $\tau = 1$ indicates the grain. We have also introduced the small parameter

$$h = \frac{e}{2C} + \varphi = \frac{e}{2C} - V_g \ll \frac{e}{C}, \quad (11)$$

which measures deviations from the degeneracy point. Considering τ as an abstract *orbital* index, the Hamiltonian can be rewritten in a more convenient way by introducing another set of Pauli matrices for the orbital sector:^{9,17}

$$\begin{aligned} H &= \sum_{k,\tau} \epsilon_k a_{k\tau}^\dagger a_{k\tau} + ehT^z \\ &+ \sum_{k,k'} \left[\sum_{\tau,\tau'} \left(\frac{J}{2} \vec{\sigma} \cdot \vec{S} + V \right) (\tau^x T^x + \tau^y T^y)_{\tau,\tau'} a_{k\tau}^\dagger a_{k'\tau'} \right. \\ &\left. + \sum_{\tau} \left(\frac{J}{2} \vec{\sigma} \cdot \vec{S} + V \right) a_{k\tau}^\dagger a_{k'\tau} \right]. \end{aligned} \quad (12)$$

In this equation, the operators (S, σ) act on spin and the (T, τ) act on the (charge) orbital degrees of freedom.

The key role of this mapping stems from the fact that $\langle \hat{Q} \rangle$ can be identified as (an orbital pseudo-spin)

$$\langle \hat{Q} \rangle = e \left(\frac{1}{2} + \langle T^z \rangle \right). \quad (13)$$

Then, we can introduce the extra (charge) state $|Q\rangle$ as an auxiliary label to the state $|\Phi\rangle$ of the grain. In addition to introducing the label $|Q\rangle$ we make the replacement

$$\begin{aligned} a_{k1}^\dagger a_{k'0} \hat{P}_0 &\longrightarrow a_{k1}^\dagger a_{k'0} T^+ \\ a_{k0}^\dagger a_{k'1} \hat{P}_1 &\longrightarrow a_{k'0}^\dagger a_{k1} T^-. \end{aligned} \quad (14)$$

Notice that T^+ and T^- are pseudo-spin ladder operators acting only on the charge part $|Q\rangle$. More precisely, we have the correct identifications

$$\begin{aligned} T^-|Q=1\rangle &= T^-|T^z = +1/2\rangle = |Q=0\rangle \\ T^+|Q=0\rangle &= T^+|T^z = -1/2\rangle = |Q=1\rangle, \end{aligned} \quad (15)$$

meaning that the charge on the single-electron box is adjusted whenever a tunneling process takes place. Furthermore, since $T^+|Q=1\rangle = 0$ and $T^-|Q=0\rangle = 0$ these operators ensure in the same way as the projection operators \hat{P}_0 and \hat{P}_1 that only transitions between states with $Q=0$ and $Q=1$ take place. This leads us to identify $\hat{P}_1 + \hat{P}_0$ with the identity operator on the space spanned by $|0\rangle$ and $|1\rangle$ and $\hat{P}_1 - \hat{P}_0$ with $2T^z$. We now introduce an additional pseudo-spin operator via:

$$\begin{aligned} a_{k1}^\dagger a_{k'0} &= \frac{1}{2} a_{k\tau}^\dagger \tau^- a_{k'\tau'} \\ a_{k0}^\dagger a_{k'1} &= \frac{1}{2} a_{k\tau}^\dagger \tau^+ a_{k'\tau'}, \end{aligned} \quad (16)$$

where the matrices $\tau^\pm = \tau^x \pm i\tau^y$ are standard combinations of Pauli matrices. Finally, the Coulomb term h mimics a magnetic field acting on the orbital space. Therefore, the (quantum) grain capacitance $C_g = -\partial\langle \hat{Q} \rangle / \partial h$ is equivalent to the local isospin susceptibility $\chi_T = -\partial\langle T^z \rangle / \partial h$ up to a factor e . For simplicity, we will subtract the classical contribution C which is V_g -independent.

But obviously, to compute the latter, we have to determine the nature of the Kondo ground state exactly.

Typically, when only ‘‘charge flips’’ are involved through the V term, the model can be mapped onto a two-channel Kondo model (the two channels correspond to the two spin states of an electron), and the capacitance always exhibits a *logarithmic divergence* at zero temperature.⁹ Here, we have a combination of spin and charge flips. Can we then expect two distinct energy scales for the spin and orbital sectors? To answer this question, we perform a perturbative scaling analysis following that of a related model in Ref. [36]. We first rewrite the interacting part of the Hamiltonian in real space as:

$$\begin{aligned} H_K &= \frac{J}{2} \vec{S} \cdot (\psi^\dagger \vec{\sigma} \psi) \\ &+ \frac{V_\perp}{2} T^z (\psi^\dagger \tau^z \psi) + \frac{V_\perp}{2} [T^+ (\psi^\dagger \tau^- \psi) + h.c.] \\ &+ Q_z T^z \vec{S} \cdot (\psi^\dagger \tau^z \vec{\sigma} \psi) + Q_\perp \vec{S} \cdot [T^+ (\psi^\dagger \tau^- \vec{\sigma} \psi) + h.c.], \end{aligned} \quad (17)$$

where $\psi_{\tau\sigma} = \sum_k a_{k\tau\sigma}$.

A host of spin-exchange \otimes isospin-exchange interactions are clearly generated; J refers to pure spin-flip processes involving the $S=1/2$ spin of the small dot, V_\perp to pure charge flips which modify the grain charge, and Q_\perp describes exotic spin-flip assisted tunneling.

This Hamiltonian exhibits a structure which is very similar to the one introduced in Ref. [26] in order to study a symmetrical double (small) quantum dot structure with strong capacitive coupling.²⁶ However, since the physical situation that led us to this Hamiltonian here is very different from that of Ref. [26], our bare values for the coupling parameters are also very different (for $J \ll 1$):

$$V_\perp = V, \quad V_z = 0, \quad Q_z = 0, \quad Q_\perp = J/4. \quad (18)$$

We have ignored the potential scattering $V\psi^\dagger\psi$ which does not renormalize. It is also relevant to note that this model belongs to the general class of problems of two coupled Kondo impurities. However the coupling between impurities, namely Q_\perp , is far different from the more usual RKKY interaction.³⁷

Again, bear in mind that here the operators $\hat{P}_{1,0} = (1 \pm 2T^z)/2$ and $\hat{p}_{0,1} = (1 \pm \tau^z)/2$ project out the grain state with $Q = e$ and $Q = 0$, and the reservoir/grain electron channels, respectively. The spin \vec{S} corresponds to the spin of the small dot in the Kondo regime and the index σ is the spin state of an electron in the reservoir or in the grain.

Note that in the situation of Ref. [26], the operators $\hat{P}_\pm = (1 \pm 2T^z)/2$ and $\hat{p}_\pm = (1 \pm \tau^z)/2$ rather project out the small double dot states $(n_+, n_-) = (1, 0)$ and $(0, 1)$, and the right/left (+/-) lead channels, respectively. Additionally, the spin \vec{S} is the spin (excess) impurity either on the left or the right dot and the index σ denotes the spin state of electrons in the reservoirs. The corresponding bare values in that case would be rather of the form:

$$V_\perp = Q_\perp, V_z, Q_z = J. \quad (19)$$

B. Perturbative Renormalization Group analysis

The low-energy Hamiltonian can be treated using perturbative renormalization group (RG). It is relevant to observe that no new interaction terms are generated to second order as the bandwidth is reduced. By integrating out conduction electrons with energy larger than a scale $E \ll D$ ($\sim \min\{E_c, \Delta_d\}$ being either the level spacing of the small dot or the charging energy of the grain, i.e., the ultraviolet cutoff), we obtain at second order the following RG equations for the five dimensionless coupling constants:

$$\begin{aligned} \frac{dJ}{dl} &= J^2 + Q_z^2 + 2Q_\perp^2 \\ \frac{dV_z}{dl} &= V_\perp^2 + 3Q_\perp^2 \\ \frac{dV_\perp}{dl} &= V_\perp V_z + 3Q_\perp Q_z \\ \frac{dQ_z}{dl} &= 2JQ_z + 2V_\perp Q_\perp \\ \frac{dQ_\perp}{dl} &= 2JQ_\perp + V_z Q_\perp + V_\perp Q_z, \end{aligned} \quad (20)$$

with $l = \ln[D/E]$ being the scaling variable, E is the running bandwidth. This RG analysis is applicable only very close to the degeneracy point $\varphi = -e/(2C)$ where the effective Coulomb energy in the grain or h vanishes and obviously only when all coupling constants stay $\ll 1$. Higher orders in the RG have been neglected.

Although the equations (20) have no simple analytic solution, one can try to read off the essential physics from numerical integration and the initial conditions (18).

Let us first discuss the most obvious case of a particle-asymmetric level, with $V_\perp > 0$ meaning (large) $U \gg -2\epsilon$. In this case, the numerical integration of the RG flow indicates that even though we start with completely *asymmetric* bare values of the coupling constants, all couplings diverge at the same energy scale due to the presence of the spin-flip assisted tunneling terms Q_\perp and Q_z . This energy scale that we can identify with a generalized Kondo temperature is difficult to calculate analytically. However, we can approximate it by the one of the completely symmetrical model

$$T_K^{SU(4)} \sim D e^{-1/4J}. \quad (21)$$

Furthermore, we have checked numerically that all coupling ratios converge to one in the low energy limit provided the RG equations can be extrapolated in this regime. These results have been summarized in Figure 2. As confirmed below with an exact Numerical RG treatment, the entanglement of spin and orbital degrees of freedom in this geometry will lead to a higher symmetry than $SU(2) \otimes SU(2)$, namely $SU(4)$, and then to the formation of a Fermi-liquid correlated ground-state with, e.g., the complete screening of the orbital spin \vec{T} . [$SU(4)$ is the minimal group allowing spin-orbital entanglement and which respects rotational invariance both in spin and orbital spaces.] Recall that the presence of the spin-flip assisted tunneling terms then definitely hinders the possibility of a non-Fermi liquid ground state induced by the over-screening of the the pseudo-impurity \vec{T} .

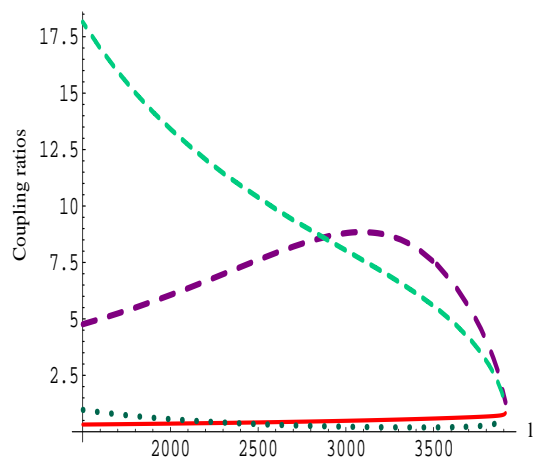


FIG. 2: Evolution of the four coupling ratios as a function of the scaling variable $l = \ln(D/E)$. The initial conditions have been chosen as: $J(0) = u$, $V_\perp(0) = 0.10u$, $Q_\perp(0) = u/4$ with $u = 0.00018$ and $V_z(0) = Q_z(0) = 0$. The full line is Q_\perp/J , the dotted line V_\perp/V_z , and the dashed lines to Q_\perp/V_\perp and Q_\perp/Q_z (which diverges for $l \rightarrow 0$). All the couplings are strongly renormalized for $l_c \approx 3914$ and all their ratios converge to 1. Extrapolating the flow to $l \gg l_c$ would give a straight horizontal line where the coupling ratios remain 1.

Let us now analyze the particle-hole symmetric case, i.e., $V_\perp = 0$. At second order, the RG flow would tend to suggest that two parameters, namely V_\perp and Q_z remain *zero* whatever the energy scale. Typically, the Kondo coupling J is the largest throughout the RG flow and seems to be the first one to diverge. On the other hand, the ratios V_z/J and Q_\perp/J cannot be neglected which tends to exclude an $SU(2) \times SU(2)$ symmetry where the spin and the orbital degrees of freedom would be independently screened (Figure 3). Instead, spin-orbital mixing (entanglement) seems to be prominent at low-energy. Even though the perturbative RG is certainly not sufficient to draw more definitive conclusions, it is also instructive to observe that for $V_\perp < 0$, the ratios Q_\perp/J and V_z/J still converge to one. Since the system definitely has to restore the rotational invariance both in spin

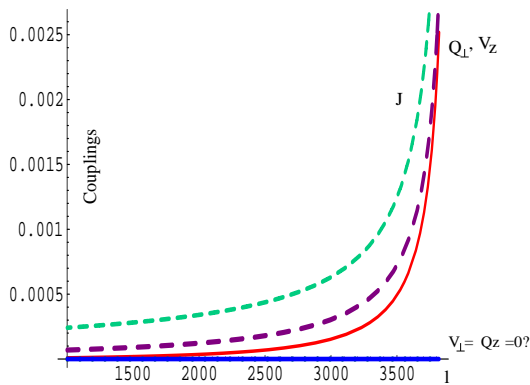


FIG. 3: Here, we have chosen: $J(0) = u$, $Q_{\perp}(0) = u/4$ with $u = 0.00018$ and $V_{\perp}(0) = V_z(0) = Q_z(0) = 0$. The coupling $J(l)$ is the largest throughout the RG flow, but the ratios Q_{\perp}/J and V_z/J cannot be neglected. Furthermore, at second order, the couplings V_{\perp} and Q_z would remain zero. However, the NRG concludes that even in this limit the system converges to an $SU(4)$ Fermi-liquid fixed point with identical coupling constants which emphasizes the importance of higher-order terms and that spin-orbital mixing is well prominent and that the rotational invariance is restored both in spin and orbital spaces.

and orbital spaces, this tends to emphasize that higher-order terms play a crucial role in the crossover regime eventually by restoring an $SU(4)$ Fermi-liquid even for those cases. Moreover, the RG analysis suggests that the temperature scale at which the Fermi-liquid behavior emerge would be much smaller for vanishing and negative V_{\perp} because the system needs a much longer time to restore the rotational symmetry both in spin and orbital spaces. To enumerate higher order terms would be a very tedious task, therefore this assertion will be rather checked by NRG, a completely non perturbative method. To summarize this part, we emphasize that for $V_{\perp} \leq 0$, the above perturbative analysis does not allow us to determine the precise nature of the low-temperature fixed point, whether the orbital (isospin) moment is exactly screened or over-screened. We will prove in section IV E using NRG, that a $SU(4)$ strongly-correlated ground state emerges for any physical value of V_{\perp} , i.e., $-J/4 \leq V_{\perp} \leq J/4$.

C. Entanglement of spin and charge degrees of freedom

This RG analysis suggests – at least for not too small positive V_{\perp} – that our model becomes equivalent at low energy to an $SU(4)$ *symmetrical* exchange model:

$$H_K = J \sum_A \psi_{\mu}^{\dagger} t_{\mu\nu}^A \left[\sum_{\alpha\beta} \left(S^{\alpha} + \frac{1}{2} \right) \left(T^{\beta} + \frac{1}{2} \right) \right]^A \psi_{\nu} \quad (22)$$

$$= \frac{J}{4} \sum_A M^A \sum_{\mu,\nu} \psi_{\mu}^{\dagger} t_{\mu\nu}^A \psi_{\nu}.$$

Since all the coupling ratios converge to one, we have rewritten the Kondo Hamiltonian (17) with the unique coupling constant J . We have introduced the “hyper-spin”

$$M^A \in \{2S^{\alpha}, 2T^{\alpha}, 4S^{\alpha}T^{\beta}\}, \quad (23)$$

for $\alpha, \beta = x, y, z$. The operators M^A can be regarded as the 15 generators of the $SU(4)$ group. Moreover, this conclusion will be strongly reinforced by the NRG analysis proposed below (whose range of validity is broader than Eqs. (20)) which indeed concludes that the effective Hamiltonian (22) is appropriate for all values of $-J/4 \leq V_{\perp} \leq J/4$. Note that apparently (22) has $SU(2) \times SU(2)$ symmetry, representing rotational invariance in both spin and orbital (pseudo-spin) spaces, and also interchange symmetry between spin and pseudo-spin. But, the full symmetry is actually the higher symmetry group $SU(4)$, which clearly unifies (entangles) the spin of the small dot and the charge degrees of freedom of the metallic grain. Notice that the irreducible representation of $SU(4)$ written in Eq. (22) has been used previously for spin systems with orbital degeneracy.^{38,39} The electron operator ψ now transforms under the fundamental representation of the $SU(4)$ group, with generators $t_{\mu\nu}^A$ ($A = 1, \dots, 15$), and the index μ labels the four combinations of possible spin (\uparrow, \downarrow) and orbital indices $(0, 1)$, which means $(0, \uparrow)$, $(0, \downarrow)$, $(1, \uparrow)$ and $(1, \downarrow)$.

The emergence of such a strongly-correlated $SU(4)$ ground state, characterized by the quenched hyper-spin operator

$$\left(\vec{S} + \frac{1}{2} \right) \left(\vec{T} + \frac{1}{2} \right), \quad (24)$$

clearly reflects the strong *entanglement* between the *charge* degrees of freedom of the *grain* and the *spin* degrees of freedom of the *small dot* at low energy induced by the prominence of spin-flip assisted tunneling. There is the formation of an $SU(4)$ Kondo singlet which is a singlet of the spin operator, the orbital operator, and the orbital-spin mixing operator $U^{\alpha,\beta} = S^{\alpha}T^{\beta}$. Again, let us argue that this enlarged symmetry arises whatever the parameter V_{\perp} simply because the spin-flip assisted tunneling term Q_{\perp} always flows off to strong couplings at the same time than the more usual Kondo term J ; The system then must inevitably converge to a fixed point with orbital-spin mixing. To respect rotational invariance in both spin and orbital spaces the only possibility is indeed an $SU(4)$ -symmetric Kondo model (as agreed with NRG).

D. Capacitance: Destruction of Matveev’s logarithmic singularity

The (one-channel) $SU(N)$ Kondo model has been extensively studied in the literature (see, e.g., Ref. [40]).

In particular, the strong coupling regime corresponds to a *dominant* Fermi liquid fixed point induced by the complete screening of the hyper-spin M^a , implying that all the generators of $SU(4)$ yield a local susceptibility with a behavior in⁴¹ $\sim 1/T_K^{SU(4)}$. T^z being one of these generators, we deduce that $\chi_T = -\partial\langle T^z \rangle / \partial h$ and then the (quantum) capacitance of the grain $C_q = -\partial\langle \hat{Q} \rangle / \partial h$ roughly evolves as $1/T_K^{SU(4)}$ at low temperatures;⁴¹ We have subtracted the classical capacitance C . Consequently, for $h \ll e/C$, we obtain a linear dependence of the average grain charge as a function of $V_g = -\varphi$:

$$\langle \hat{Q} \rangle - \frac{e}{2} = -e \frac{h}{T_K^{SU(4)}} = -\frac{e}{T_K^{SU(4)}} \left[\frac{e}{2C} + \varphi \right]. \quad (25)$$

The hallmark of the formation of the $SU(4)$ Fermi liquid in our setup is now clear. The (grain) capacitance peaks are completely smeared out by the mixing of spin and charge flips and Matveev's logarithmic singularity⁹ has been completely destroyed. Additionally, the strong renormalization of the V (and J) term – and the stability of the strong-coupling Kondo fixed point – clearly reflects that the effective transmission coefficient between the lead and the grain becomes maximal close to the Fermi level. (The maximum of the tunneling appears not exactly at the Fermi level as one could guess from the value of the phase shifts $\delta = \pi/4$.)

This example could also be interpreted as an interesting proof that one can already wash out the Coulomb staircase when the ‘effective’ transmission coefficient between the grain and the lead is roughly one only close to the Fermi energy (and not for all energies²⁵). Conceptually, this is not accessible with a small dot in the resonant level limit.^{22,24} *We stress that this stands for a remarkable signature of the formation of a Fermi-liquid ground state when tunneling through a single-electron box.*

E. Confirmation with Numerical Renormalization Group analysis

In order to confirm the results obtained by perturbative RG and extend our investigation to the strong coupling regime, we have performed a collaborative NRG^{33,42} analysis of the model described by Eq. (17) similar as in Ref. [26]. Note in passing that the model of Eq. (17) with asymmetric bare values is not strictly speaking integrable. Therefore, we resort to the NRG method which in general can be successfully applied to (various) two-impurity Kondo models.⁴³ At the heart of the NRG approach is a logarithmic energy discretization of the conduction band around the Fermi points. In this method – after the logarithmic discretization of the conduction band and a Lanczos transformation – one defines a sequence of discretized Hamiltonians, H_N , with the relation:⁴²

$$H_{N+1} \equiv \Lambda^{1/2} H_N + \sum_{\tau\sigma} \xi_N \left(f_{N,\tau\sigma}^\dagger f_{N+1,\tau\sigma} + \text{h.c.} \right), \quad (26)$$

where $f_{0,\tau\sigma} = \psi_{\tau\sigma} / \sqrt{2}$ and $H_0 \equiv 2\Lambda^{1/2} / (1 + \Lambda) H_K$ with $\Lambda \sim 3$ as discretization parameter, and $\xi_N \approx 1$. For the definition of f_N see Ref. [42]. The original Hamiltonian is connected to the H_N 's as $H = \lim_{N \rightarrow \infty} \omega_N H_N$ with $\omega_N = \Lambda^{-(N+1)/2} (1 + \Lambda) / 2$. Using the logarithmic separation of the energy scales we are allowed to diagonalize H_N 's iteratively and calculate physical quantities directly at the energy scale $\omega \sim \omega_N$. We have calculated the dynamical spin and orbital spin (ac) susceptibilities

$$\Im m \chi_{\mathcal{O}}(\omega) = \Im m \mathcal{F}[\langle \mathcal{O}(t), \mathcal{O}(0) \rangle], \quad (27)$$

where $\mathcal{O} = T^z, S^z$ and \mathcal{F} denotes the Fourier transform. According to the discussion above, the couplings were chosen as $J = 4Q_\perp$, $Q_z = V_z = 0$.

The obtained orbital spin susceptibility for different values of V_\perp is shown in Figure 4. Regardless of the value of V_\perp , the T^z susceptibility exhibits a typical Fermi-liquid like peak at an energy scale which can be identified as $T_K^{SU(4)}$. Above this energy scale it behaves as $\chi \sim \omega^{-1}$ indicating that the correlation function in Eq. (27) is constant for very short times while for $\omega < T_K^{SU(4)}$, $\chi \sim \omega$ as a signature of the $\sim 1/t^2$ asymptotic of the aforementioned correlation function for a Fermi-liquid model. Indeed, at $T=0$, this ensures a grain's capacitance,

$$C_q = \int_{1/T_K^{SU(4)}}^{+\infty} dt \langle [T^z(t), T^z(0)] \rangle = \frac{1}{T_K^{SU(4)}}. \quad (28)$$

Furthermore, as one can see in Figures 4, 6 (for $\Delta_z \rightarrow 0$) the Kondo screening simultaneously takes place in the spin and orbital sectors, indicating the $SU(4)$ -symmetric nature of the effective low energy Hamiltonian.

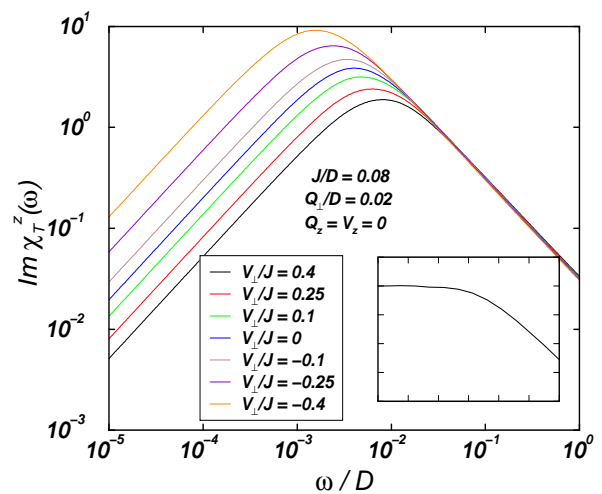


FIG. 4: The orbital spin T^z susceptibility for different values of V_\perp . In all the cases the susceptibility shows a typical $SU(4)$ Fermi-liquid state at $\omega = T_K^{SU(4)}(V_\perp)$. *Inset*: As a comparison we plot the same quantity for the 2-channel Kondo model. Furthermore, we can clearly observe that $T_K^{SU(4)}$ markedly decreases for lower values of U meaning $V_\perp/J < 0$ (i.e., by making the small dot larger and larger.⁴⁴)

To give a rigorous proof of the $SU(4)$ Fermi liquid ground state one has to analyze the finite size spectrum obtained by NRG. It turns out that (as in Ref. [26]) the spectrum can be understood as a sum of four independent chiral fermion spectra with phase shift $\pi/4$ in accordance with the prediction of the $SU(4)$ Fermi liquid theory. This result proves that the low-energy behavior is described by the Fermi liquid theory even at $V_{\perp} = 0$, but as conjectured above the temperature scale at which the Fermi liquid emerges decreases as we change the coupling V_{\perp} from $0.4J$ to $-0.4J$.

For comparison, in the inset of Figure 4 we plot the dynamical susceptibility for the two channel Kondo model: In that case, $\Im m \chi(\omega) \sim \text{const.}$ which in contrast traduces that the capacitance C_q would exhibit a logarithmic divergence at zero temperature.⁹

Additionally, the $SU(4)$ Kondo temperature scale is considerably reduced for negative values of V_{\perp} , i.e., by decreasing the on-site interaction U on the small dot ($U \ll -2\epsilon$). This makes sense since by substantially decreasing the Coulomb energy of the small dot – i.e., by progressively increasing the size of the small dot – one expects the breakdown of the $SU(4)$ fixed point and a situation similar to that of a reservoir and *two* large dots⁴⁴ (According to Eq. (2), spin Kondo physics should definitely vanish for $U \ll -\epsilon$).

V. ON THE STABILITY OF THE $SU(4)$ FIXED POINT AND CROSSOVERS

In contrast to the two-channel Kondo fixed point, which is known to be extremely fragile with respect to perturbations (e.g., channel asymmetry, magnetic field), the $SU(4)$ fixed point is robust at least for *weak* perturbations.

In order to demonstrate the robustness of the $SU(4)$ Fermi liquid fixed point we have checked the role, e.g., of a magnetic field in real and orbital spin sectors. It turns out that both terms are marginal operators in RG sense. On the other hand, when the magnetic [orbital] field is much larger than the scale of the Kondo temperature, the processes which involve spin [orbital spin] flips are suppressed and low energy physics is described by a *one-channel* orbital spin [spin] Kondo effect, with a smaller Kondo temperature than that of the $SU(4)$ case. Let us now thoroughly analyze the different fixed points, the effects of an asymmetry between the tunnel junctions and of rather large junctions with more conducting channels.

A. Magnetic field

First of all, we have checked with NRG that the $SU(4)$ Fermi liquid fixed point resists for quite weak external magnetic field. But, applying a *strong* magnetic field $B \gg T_K$ unavoidably destroys the $SU(4)$ symmetry. But

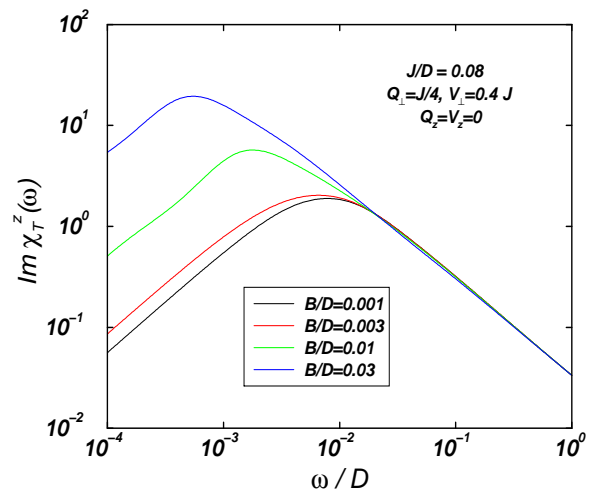


FIG. 5: The orbital spin T^z susceptibility for different values of the external magnetic field B . The low-energy physics consists of a Fermi liquid regardless of B , but the symmetry is reduced for large magnetic fields to $SU(2)$ (for the orbital space) and the Kondo energy scale as well.

at zero temperature, we expect the behavior of charge fluctuations close to the degeneracy points to remain qualitatively similar. Indeed, in a large magnetic field spin flips are suppressed at low temperatures, i.e., $Q_{\perp} = Q_z = J = 0$, and the orbital degrees of freedom, through V_{\perp} and V_z , develop a standard one-channel Kondo model (the electrons have only spin-up or spin down), which also results in a Fermi-liquid ground state with a linear dependence of the average grain charge as in Eq. (25). Yet, the emerging Kondo temperature will be much smaller,

$$T_K[B = \infty] \approx D e^{-1/V}, \quad (29)$$

with for instance $V \approx t^2/(-2\epsilon)$ for $U \rightarrow +\infty$, and might not be detectable experimentally. A substantial decrease of the Kondo temperature when applying an external magnetic field B has also been certified using NRG even for extremely large values of V (Figure 5).

B. Away from the degeneracy points: small dot as a resonant level

A weak orbital magnetic field (orbital splitting) $\Delta_z \propto h$ does not modify the $SU(4)$ Fermi liquid state.

Moreover, the application of a *strong* Δ_z always leads to a single-channel Kondo effect in the spin sector. A naive consideration – focusing on the RG flow above – would suggest the possibility of a two-channel (spin) Kondo effect: The simultaneous screening of the excess spin of the small dot by the lead and the grain electrons, independently. However, going back to the Schrieffer-Wolff transformation for the situation away from the degeneracy points, the charging energy of the metallic grain

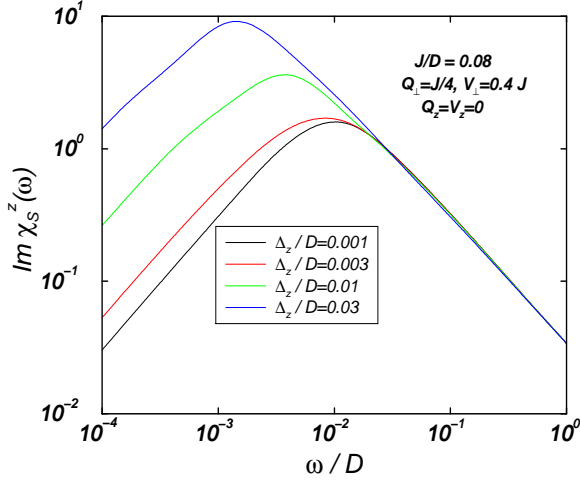


FIG. 6: The real spin S^z susceptibility for different values of the orbital splitting, Δ_z . For $\Delta_z > T_K^{SU(4)}$ the processes which involve orbital spin flip are suppressed resulting in a purely *one-channel* spin Kondo effect with a smaller Kondo temperature of the order of that for a small dot embedded between two leads $T_K[\Delta_z]$. Recall that the energy scale at which the SU(4) correlated state arises can be much larger than $T_K[\Delta_z]$ which should certainly ensure the observation of our theoretical results. It is worthwhile to note the parallel between Figures 5 and 6 by interchanging $T^z \leftrightarrow S^z$ and $\Delta_z \leftrightarrow B$ (however, $T_K[\Delta_z] > T_K[B]$).

definitely ensures $J_1 \neq J_0$ (provided we start with almost symmetric junctions), a condition that destroys the stability of the two-channel spin Kondo fixed point. The spin Kondo coupling J_0 will be the first one to flow off to strong couplings (as anticipated in Section III). The NRG calculation clearly confirms this expectation: the Δ_z term not only suppresses the orbital spin-flip terms but also generates an asymmetry between the grain-dot and lead-dot spin couplings which destroys the two-channel Kondo behavior. The possible two-channel (spin) Kondo regime proposed by Oreg and Goldhaber-Gordon³⁵ can not be reached with this model, at least, for symmetric junctions. Asymmetric junctions and a fine tuning of the grain gate voltage far from the degeneracy points would be necessary to reach the condition $J_0 = J_1$. On the other hand we will see that, for quite asymmetric barriers, a two-channel Kondo behavior rather for the orbital degrees of freedom can appear near the degeneracy points but at extremely small (and *a priori* unreachable) temperatures.

For $\Delta_z \gg T_K^{SU(4)}$, the Kondo temperature scale here resembles that for a small dot connected to two leads ($J_0 = J$)³⁴ and, in principle, is still experimentally accessible:

$$T_K[\Delta_z] \sim D e^{-1/J} < T_K^{SU(4)}. \quad (30)$$

Henceforth, this will cutoff the logarithmic divergence in the charge fluctuations away from the degeneracy point

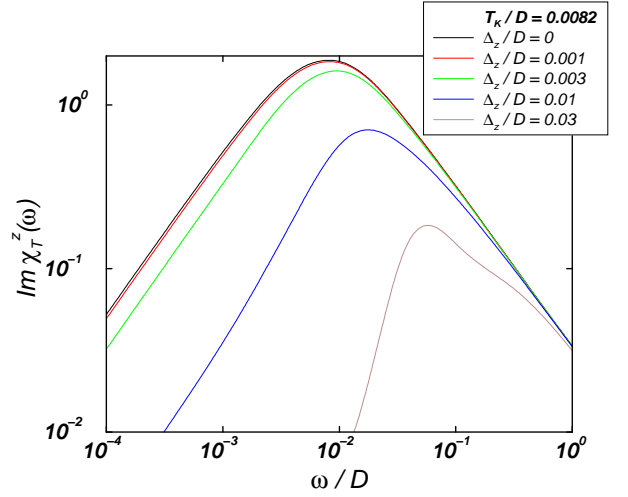


FIG. 7: The orbital spin T^z susceptibility for different values of the orbital splitting, Δ_z . For $\Delta_z > T_K^{SU(4)}$ the processes which involve orbital spin flip are clearly suppressed at a scale of Δ_z producing instead a Schottky anomaly. The orbital pseudospin model then becomes inappropriate to describe the charge fluctuations of the grain at low energy. We rather apply another resonant level mapping and a perturbation theory similar to that of Ref. [24].

$\varphi = -e/2C$ [see Eq. (9)]. In order to describe the physics at strong orbital magnetic field, i.e., away from the degeneracy points and at lower temperature and more precisely the average grain charge $\langle Q \rangle$, we seek to go beyond the effective model in Eq. (17). Indeed, at energy smaller than $T_K[\Delta_z]$, the physics can be qualitatively identified with that of Ref. [24]: The Kondo screening of the excess spin of the small dot by the lead produces an Abrikosov-Suhl resonance at the Fermi level, and the small dot plus the lead can be replaced by a resonant level with the energy $\epsilon \rightarrow 0$ and the resonance width $\sim T_K[\Delta_z]$. Now, one can still allow for a (weak) residual tunneling matrix element \hat{t} between the grain and the effective resonant level (which may be of the same order as the bare tunneling matrix element t between the small dot and the grain but its value is difficult to determine accurately). For an illustration, see Figure 8. Reformulating results of Ref. [24] for our case and including that $T_K[\Delta_z] \ll U_1, U_{-1}$ for $N = CV_g/e \ll 1/2$ ($\varphi \ll -e/2C$), at zero temperature we find

$$\begin{aligned} \langle Q \rangle &= e \frac{\Gamma}{\pi} \left(\frac{1}{U_1} - \frac{1}{U_{-1}} \right) \\ &= e \frac{\Gamma}{E_c \pi} \frac{4N}{(1-2N)(1+2N)}, \end{aligned} \quad (31)$$

with the effective tunneling energy scale

$$\Gamma = \pi \sum_p \hat{t}^2 \delta(\epsilon_p) \ll U_1, U_{-1}. \quad (32)$$

Since U_1 and U_{-1} are of the order of E_c for $N \ll 1/2$, we observe that the charge smearing far from the degeneracy

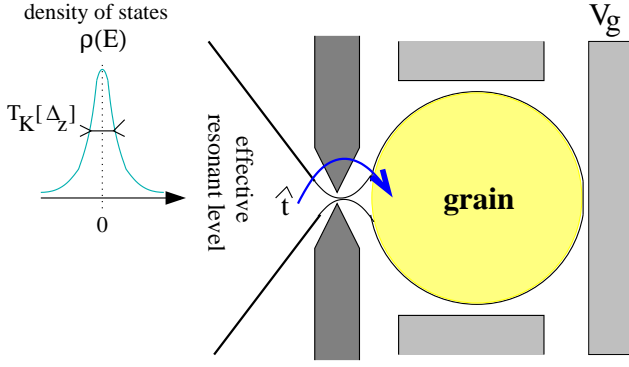


FIG. 8: Illustrative view of the effective low-energy model for almost symmetric barriers away from the degeneracy points: According to Eq. (6) the charging energy on the grain inevitably ensures that the spin Kondo coupling J_0 between the bulk lead and the small dot will be the first one to flow off to strong couplings at the energy scale $T_K[\Delta_z]$. The grain becomes virtually weakly-coupled to an effective *resonant level* with a reduced bandwidth $\sim T_K[\Delta_z] \ll D$.

points is small at low temperatures. Additionally, recall that for $N \ll 1/2$ and zero temperature, at second order in \hat{t} the average grain charge also exhibits a (small) linear behavior as a function of N or V_g which is slightly distinct from the original Matveev's situation (Figure 9).^{9,10}

C. Case of asymmetric junctions

Another interesting perturbation is the explicit symmetry breaking between the dot-lead and dot-grain tunneling amplitudes. To address this issue, it is convenient to rewrite the Kondo Hamiltonian in the most general form as follows (again $\tau = 0$ for the bulk lead and $\tau = 1$ for the grain):

$$\begin{aligned}
 H_K = & \sum_{\tau=0,1} \left(J_\tau \psi_\tau^\dagger \vec{S} \cdot \frac{\vec{\sigma}}{2} \psi_\tau \right) \\
 & + \sum_{\tau=0,1} \left(\frac{1}{2} (-1)^\tau V_{z,\tau} T^z \psi_\tau^\dagger \psi_\tau \right) \\
 & + \frac{V_\perp}{2} [T^+ (\psi^\dagger_{\tau^-} \psi) + h.c.] \\
 & + \sum_{\tau=0,1} \left(Q_{z,\tau} (-1)^\tau T^z \vec{S} \cdot (\psi_\tau^\dagger \vec{\sigma} \psi_\tau) \right) \\
 & + Q_\perp \vec{S} \cdot [T^+ (\psi^\dagger_{\tau^-} \vec{\sigma} \psi) + h.c.].
 \end{aligned} \tag{33}$$

The corresponding bare values are embodied by

$$\begin{aligned}
 J_0 = J, \quad J_1 = K^2 J, \quad Q_\perp = \frac{KJ}{4} \\
 V_\perp = VK, \quad Q_{z,\tau} = V_{z,\tau} = 0,
 \end{aligned} \tag{34}$$

where we have introduced the asymmetry parameter $K = t_1/t$; $t = t_0$ (t_1) denotes the hopping amplitude between the lead (grain) and the small dot. Since the asymmetry stands for a marginal perturbation in the RG sense

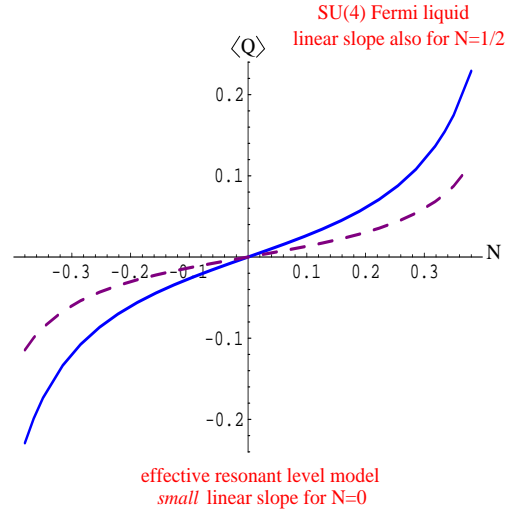


FIG. 9: Profile of the average charge $\langle Q \rangle$ on the grain versus $N = CV_g/e$ for (almost) symmetric junctions and $T < T_K[\Delta_z]$. Again, the SU(4) Kondo entanglement between spin and orbital degrees of freedom, e.g., at the degeneracy point $N = 1/2$ produces a Fermi-liquid state and the Coulomb staircase exhibits a conspicuous smearing. Away from the degeneracy points, the physics becomes similar to that of a resonant level weakly coupled to a grain which also ensures a linear (but small) behavior for $\langle Q \rangle[N]$ when $N \rightarrow 0$; The full line curve corresponds to $\Gamma/E_c = 0.15$ and the dashed line curve to $\Gamma/E_c = 0.1$.

it is natural to argue that the SU(4) correlated ground state is still robust for weak asymmetry between the tunnel junctions. But, to obtain more quantitative results we yet resort to NRG (Figure 10). By taking $V_\perp = 0.1J$, we can observe that the mixing of spin and orbital degrees of freedom may survive until $K \approx 0.95$; This guarantees an anisotropy of roughly 10% between the conductances at the tunnel junctions to preserve the SU(4) fixed point. Mostly, the magnetic moment \vec{S} and the isospin \vec{T} are simultaneously quenched and again the spectrum can be understood as a sum of four independent chiral fermion spectra with phase shift $\pi/4$.

Let us now discuss the case of a quite *strong* asymmetry between the tunnel junctions. For completeness, we also provide the RG equations at second order for this generalized situation

$$\begin{aligned}
 \frac{dJ_\tau}{dl} &= J_\tau^2 + (Q_{z,\tau})^2 + 2Q_\perp^2 \\
 \frac{dV_{z,\tau}}{dl} &= V_\perp^2 + 3Q_\perp^2 \\
 \frac{dV_\perp}{dl} &= \frac{1}{2}V_\perp (V_{z,0} + V_{z,1}) + \frac{3}{2}Q_\perp (Q_{z,0} + Q_{z,1}) \\
 \frac{dQ_{z,\tau}}{dl} &= 2J_\tau Q_{z,\tau} + 2V_\perp Q_\perp \\
 \frac{dQ_\perp}{dl} &= Q_\perp (J_0 + J_1) + \frac{1}{2}Q_\perp (V_{z,0} + V_{z,1})
 \end{aligned} \tag{35}$$

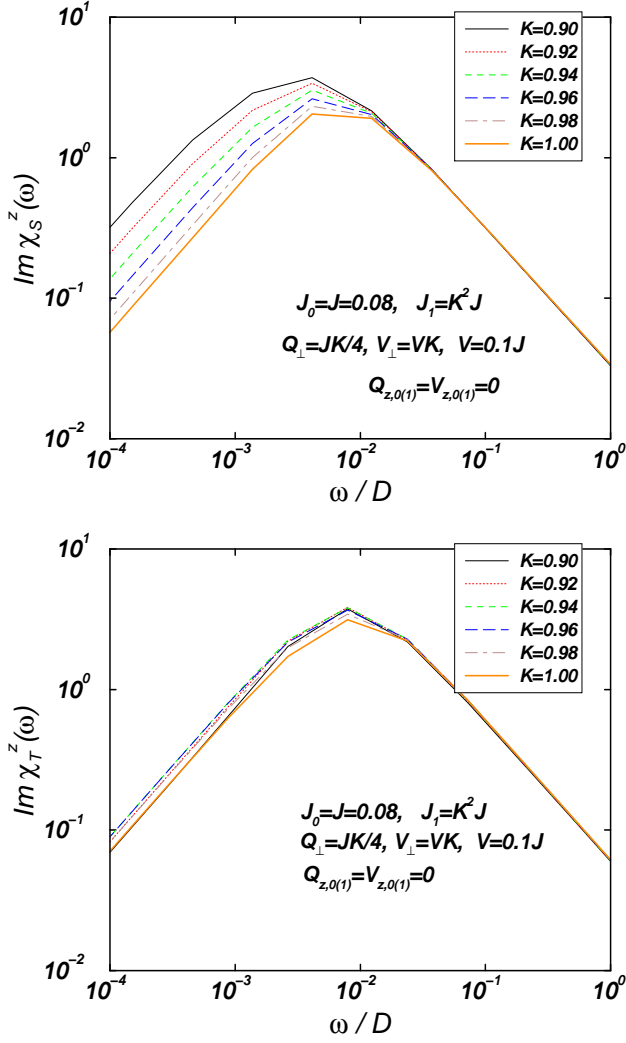


FIG. 10: Magnetic and orbital susceptibilities versus ω/D for close to unity values of the asymmetry parameter $K = t/t_1$ between the two tunnel junctions. The SU(4) ground state is stable against the inclusion of a weak asymmetry between tunnel junctions.

$$+ \frac{1}{2} V_{\perp} (Q_{z,0} + Q_{z,1}).$$

At second order, note the equality $V_{z,0}(l) = V_{z,1}(l) = V_z(l)$ regardless of the parameter K . Primarily, it is immediate to observe that for $K = 1$, we recover the previous SU(4) Fermi-liquid flow. Now we greatly diminish the tunneling amplitude between the grain and the small dot, i.e., $t_1 \ll t$ (t being fixed) and $K \ll 1$. With the present notations, it is clearly transparent that the spin Kondo coupling $J_0 = J$ between the bulk lead and the small dot will be the largest one through the RG flow and becomes of order unity at the temperature $T_K[K \ll 1] \sim D e^{-1/J} = T_K[\Delta_z]$ whereas *all the other couplings* are still negligible that breaks the SU(4) symmetry explicitly.

It is worth noting at this stage that the role of the

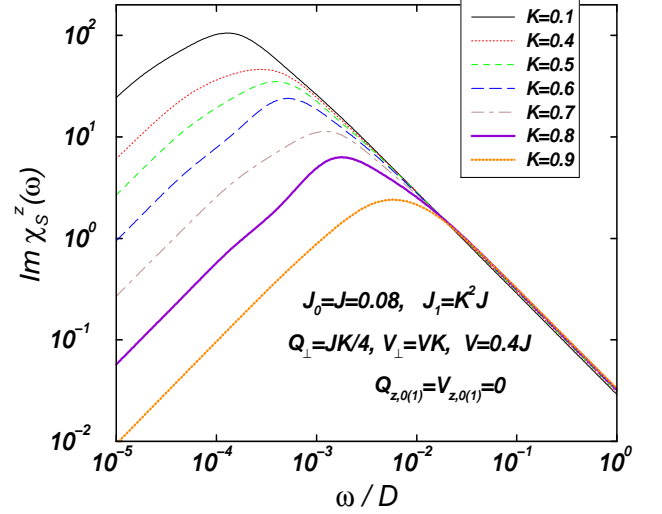


FIG. 11: Spin susceptibility versus ω/D upon increasing the asymmetry between tunneling amplitudes at the two junctions.

asymmetry parameter K seems to be practically equivalent to renormalize the orbital splitting Δ_z (compare Figures 6 and 11). The main difference however is that at the degeneracy points of the grain, one can expect a second-stage quenching of the isospin \vec{T} at some lower temperature, but obviously this (very) low-temperature regime lies much beyond the range of validity of the effective Hamiltonian (33). Furthermore, one can clearly notice that the previous perturbative result of Eq. (31) diverges if one of the charging energy U_1 or U_{-1} approaches zero, i.e., is not applicable.

In fact, as already noted in Ref. [24] it is a very difficult task to find the exact shape of the step of the staircase in the present situation of a grain at a degeneracy point coupled to an effective *resonant level*. But qualitatively, one might expect²⁴ that the physics and the resulting (two-channel) Kondo energy scale should not be so different as those of a grain coupled to a normal lead with a reduced bandwidth $T_K[K \ll 1]$, via a hopping matrix element $\hat{t} \sim t_1$:

$$T_K^{2ch} = T_K[K \ll 1] e^{-\gamma/t_1}; \quad (36)$$

Here γ is a constant parameter of the order of unity. A similar discussion should hold in the opposite regime $K \gg 1$ where one expect this time the Kondo coupling J_1 to first flow to strong coupling (since it is proportional to K^2) at the temperature scale $T_K[\Delta_z] \sim D e^{-1/J_1}$. Since the conductance between the grain and the lead is still very small at the intermediate energy scale due to the anisotropy, a second stage quenching of the orbital pseudo spin is expected at a lower energy scale in a similar manner as the case $K \ll 1$. Unfortunately for asymmetric junctions, it is difficult to formulate more quantitative results at low temperatures. A complete

renormalization group calculation starting with the bare Hamiltonian (1) would be necessary. This goes beyond the present analysis. Finally, let us mention that for more moderate values of U and ϵ , i.e. rather in the resonant level regime of the small dot, the NRG results of Lebanon *et al.*²² still support a two-channel Kondo crossover and the overscreening of the isospin moment in the case of asymmetric junctions.

D. Large junctions

We predict that the $SU(4)$ symmetry should be still robust for wider junctions characterized by $n > 1$ transverse channels with almost equal transmission amplitudes, however the associated Fermi-liquid typical energy scale decreases exponentially with the number of conducting modes. For instance, extending results of Ref.[21] for our geometry, we can clearly assess that there will be a *unique* ‘effective tunneling mode’ in the lead (it is some combination of the original tunneling modes in the lead) and another *unique* ‘tunneling mode in the box’ (also a linear combination combination of the original modes in the grain): The $T=0$ effective Hamiltonian of the model at the degeneracy points of the metallic dot corresponds to tunneling between these two modes only with or without spin flip of the excess spin of the small dot, and all the other modes can be neglected. This entirely justifies the emergence of an $SU(4)$ fixed point at very low temperatures even if the number of modes in the lead or in the grain is larger than one. However, the ultraviolet cutoff D at which the effective tunneling mode prevails, must be properly rescaled to²¹

$$T^*[n] = De^{-\alpha n}, \quad (37)$$

where α is of the order of unity. Unfortunately, this implies that an $SU(4)$ Kondo singlet can only occur at the much reduced Kondo temperature scale

$$T_K^{SU(4)}[n] \approx T^*[n]e^{-1/4J}. \quad (38)$$

Experimentally, in order to maximize chances for observing the $SU(4)$ Fermi liquid realm, it is then more advantageous to consider tunneling junctions with one clearly dominant conducting transverse mode.

VI. DISCUSSIONS AND CONCLUSIONS

We have determined exactly the shape of the steps of the Coulomb staircase for a grain coupled to a bulk lead through a small quantum dot in the Kondo regime. First, we mapped the problem onto a related model of two capacitively coupled small quantum dots.²⁶ Then, combining both NRG calculations with perturbative scaling approaches we have shed light on the possibility of a stable $SU(4)$ Fermi liquid fixed point occurring at the degeneracy points of the grain, where a Kondo effect appears

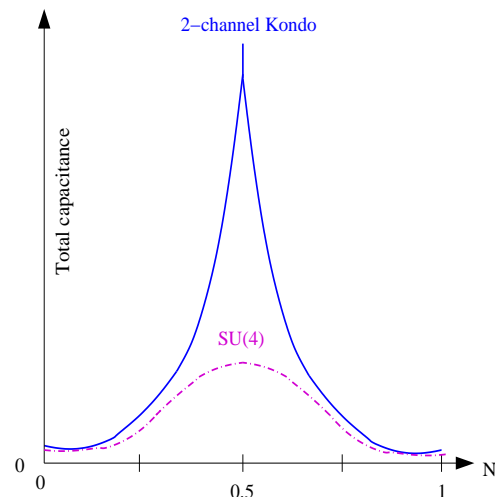


FIG. 12: Sketch of the capacitance peaks for our setup with almost symmetric junctions (dashed line) compared to those in the original Matveev’s problem (full line).⁹

simultaneously both in the spin and the orbital sectors; This demands symmetric or slightly asymmetric tunnel junctions and preferably a single-conducting channel with two spin polarizations. More generally, as in Ref. [26], these results bring precursory insight on the realization of Kondo ground states with $SU(N)$ ($N = 4$) symmetry at the mesoscopic scale.

Let us provide a physical interpretation for the occurrence of such an $SU(4)$ entanglement. Typically, close to the degeneracy points of the grain, we have two spin objects, namely the spin \vec{S} of the small dot and the orbital pseudo-spin \vec{T} of the grain depicting the two allowed degenerate charging states. Obviously, when these two spin objects are uncoupled the symmetry group of the problem is unambiguously $SU(2) \otimes SU(2)$. But, as already discussed at length in the sequel, in our setting spin-flip assisted tunneling events – i.e., an electron from the bulk lead tunnels onto the metallic grain by flipping the excess spin of the small dot and vice-versa – are very prominent at low energy; This implies that the infra-red fixed point must also reflect a visible spin-orbital mixing. *Finally, it is easy to check that $SU(4)$ is the minimal group allowing spin-orbital entanglement and which guarantees rotational invariance both in spin and orbital spaces.* Our Kondo fixed point then is rather described by the quenching of the hyper-spin $[\vec{S} + \frac{1}{2}][\vec{T} + \frac{1}{2}]$.

In a very different context, let us mention that $SU(4)$ singlets have also shown up in fermion lattice models where spin and orbital degrees of freedom play a very symmetric role.^{38,39}

The major consequence of this enlarged symmetry is that the ground state is Fermi-liquid like, which considerably smears out the Coulomb staircase behavior already in the weak tunneling region, and in particular, hinders the Matveev logarithmic singularity⁹ to take place (Figure 12). The grain capacitance exhibits instead of a loga-

rithmic singularity, a strongly reduced peak as a function of the back-gate voltage. *This stands for an irrefutable signature of the formation of a Fermi-liquid ground state when tunneling through a single-electron box.* Furthermore, we mightily emphasize that our NRG calculations markedly reproduce an SU(4) ground state regardless of the particle-hole asymmetry onto the small dot (Figure 4); More precisely, even in the case of particle-hole symmetry $2\epsilon + U = 0$, the spectrum can be still interpreted as a sum of four independent chiral fermions with phase shift $\pi/4$ in agreement with the SU(4) Fermi liquid theory. This differs from the conclusion of Ref. [22]. However, this is not so surprising in the sense that in their NRG calculations (see, e.g., their Figures 15 and 16), Lebanon *et al.* have studied a rather different limit, $U = -2\epsilon$ but $U/E_c \ll 1$, which does not correspond to our situation of a small dot and a much larger metallic grain ($U/E_c \gg 1$). Besides, in the case of symmetric barriers, they clearly noticed that a moderate Coulomb repulsion on the small dot already pushes the two-channel Kondo regime down to much lower temperature.

It is also worth to recall that the associated Kondo temperature scale $T_K^{SU(4)}$ can be strongly enhanced compared to that of the Matveev's original setup which maybe ensures the verification of our predictions. In particular, for very large U [$U \gg -2\epsilon$ and $V_\perp > 0$], $T_K^{SU(4)} \sim D \exp -(1/4J)$ may be **larger** than the Kondo scale in the conductance experiments across a single small quantum dot⁵ ($\sim 1K$), and capacitance measurements can be performed much below $100mK$.²⁰ Additionally, we have checked that the SU(4) Kondo temperature scale is considerably reduced for negative values of V_\perp , i.e., upon by (moderately) decreasing the on-site interaction U ($U \sim -\epsilon$), i.e., by making the small dot larger and larger.⁴⁴ We have carefully discussed the robustness of the SU(4) correlated state against the inclusion of *weak* perturbations like an external magnetic field, a deviation from the degeneracy points, or still an asymmetry in the tunnel junctions.

Let us now pursue and discuss an interesting crossover. So far, we have concentrated on the situation at and near the degeneracy points of the grain. Let us now apply a quite strong orbital magnetic field such that we move explicitly away from the degeneracy points. Naively, since one suppresses the orbital spin-flip terms, one could infer the emergence of a two-channel spin Kondo model through the two Kondo terms J_0 and J_1 ; However, in our setting with almost symmetric junctions, the Schrieffer-Wolff transformation away from the degeneracy points always ensures $J_0 > J_1$; The NRG calculation of Figure 6 clearly reproduces this expectation. The system then undergoes a one-channel Kondo crossover. First, the emergence of a logarithmic contribution in $\langle Q \rangle$ at quite high temperature could be potentially observable. Furthermore, at low energy, the physics resembles that of a resonant level – induced by the formation of an Abrikosov-Suhl resonance between the small dot and the bulk lead – weakly-coupled to the grain; We then recover

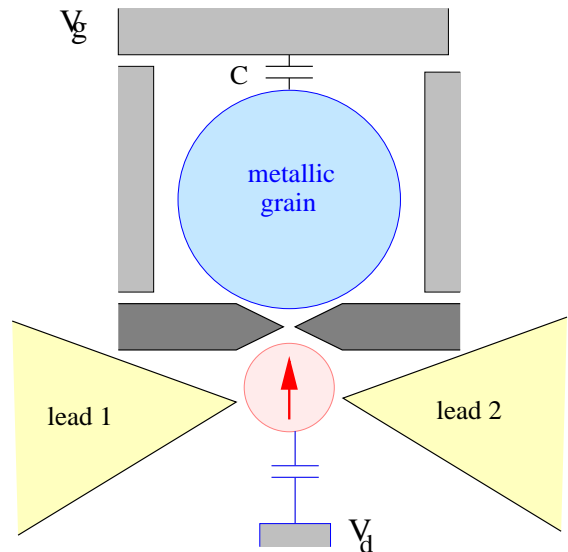


FIG. 13: Another mesoscopic double lead setup, candidate for the SU(4) model. This could be equally performed with vertically coupled dots.²⁸

a similar situation to that of Ref. [24].

Another possible realization of our SU(4) model could be still possible in a multi-lead geometry (Figure 13). Again, this would demand to be at the degeneracy points of the grain and to adjust the different tunneling junctions. More precisely, following Glazman and Raikh,³⁴ only the even linear combination of the electron creation and annihilation operators in the two bulk leads couples to the local site (small dot). The odd linear combination can be omitted and conceptually the effective model could be rewritten as in Eq. (17). Let e.g. assume that the tunnel junctions between each lead and the small dot are symmetric. Then, only the linear combination $\psi_0 = (\psi_{01} + \psi_{02})/\sqrt{2}$ will be coupled to the small dot; ψ_{0i} ($i = 1, 2$) denotes the electron annihilation operator in each lead. To recover an SU(4) Kondo fixed point, we infer that the grain-dot tunneling amplitude then must be approximately $\sqrt{2}$ times that between each lead and the small dot. This setup is particularly interesting because the capacitance of the grain and the conductance across the small dot could be both measured. Furthermore, blocking completely the opening between the grain and the small dot, one could recover a more usual Fermi liquid behavior with SU(2) spin symmetry when measuring the conductance across the small dot, and observe a net reduction of the Kondo energy scale compared to the SU(4) case due to spin orbital decoupling.

Note that this geometry – away from the degeneracy points of the grain – has been previously discussed by Oreg and Goldhaber-Gordon as a potential candidate for the appearance of a two-channel (spin) Kondo regime in a conductance measurement.³⁵ This requires meticulous fine-tuning of the gate voltages and tunnel junctions to equalize the coupling to the two channels (grain plus even

linear combination of the leads).

Definitely, the potential observation of a two-channel Kondo effect in artificial nanostructures would be an important issue^{9,45,46,47} since the emergent non-Fermi liquid behavior is very intriguing and so far difficult to observe with real magnetic impurities due to the intrinsic channel anisotropy.¹⁵ In our setting, another interesting

experiment to do in order to have potentially access to a two-channel (charge) Kondo behavior would be to stay at the degeneracy points of the grain and then progressively to shift the impurity level ϵ on the dot (which can be tuned via the gate voltage V_d of the small dot) to the Fermi energy, i.e., to reach the mixed-valence (=resonant level) limit for the small dot.²²

Acknowledgments

Part of this work was performed during the Quantum Impurity conference meeting in Dresden (April 2003). K.L.H. was supported in part by NSERC and acknowledges constructive discussions with K. Matveev. P.S. acknowledges interesting discussions with P. Brouwer, L. Glazman and P. Sharma. L.B. acknowledges the support of 'Spintronics' RT Network of the EC RTN2-2001-00440 and Hungarian Grant No. OTKA T034243.

APPENDIX A: PERTURBATIVE CALCULATIONS

Here, we derive explicitly the perturbative result of Eqs. (8) and (9). We essentially focus on the Kondo term; the perturbation theory for the direct hopping term V can be found in Ref. [9]. First, it is accurate to rewrite the Kondo term in real space as:

$$H_K = \sum_{\alpha\beta} \left[\sum_{j=0,1} \frac{J_j}{2} \vec{S} \psi_{j\alpha}^\dagger \vec{\sigma}_{\alpha\beta} \psi_{j\beta} + \frac{\tilde{J}_{10}}{2} \vec{S} \left(\psi_{0\alpha}^\dagger \vec{\sigma}_{\alpha\beta} \psi_{1\beta} + h.c. \right) \right], \quad (\text{A1})$$

where $\psi_{0\alpha} = \sum_k a_{k\alpha}$ and $\psi_{1\alpha} = \sum_p a_{p\alpha}$. The granule charge operator reads $\hat{Q} = e \sum_\alpha \psi_{1\alpha}^\dagger \psi_{1\alpha}$. Now, let $|0\rangle$ denote the ground state of the unperturbed Hamiltonian with $t = -\infty$. The first order correction $|1\rangle$ to $|0\rangle$ then reads:²⁴

$$|1\rangle = -i \int_{-\infty}^0 dt H_K(t) |0\rangle, \quad (\text{A2})$$

H_K being taken in the interaction representation. The expectation value of the charge on the dot however is second order in the Kondo coupling; Indeed, we easily get $\langle 0 | \hat{Q} | 1 \rangle = 0$. Therefore, the most leading contribution takes the form $\langle \hat{Q} \rangle_2 = \langle 0 | \hat{Q}^{(1)} | 1 \rangle$, where $\hat{Q}^{(1)}$ is the first order correction to the charge operator on the dot. This can be computed using the identification:

$$\hat{Q}^{(1)} = \int_{-\infty}^0 \hat{J}(t) dt \text{ with } \hat{J}(t) = i[H_K, \hat{Q}]. \quad (\text{A3})$$

\hat{J} must be identified as the effective current operator mediated by the Kondo coupling. This results in

$$\hat{Q}^{(1)} = ie \frac{\tilde{J}_{10}}{2} \sum_{\alpha\beta} \int_{-\infty}^0 dt \left[\vec{S} \psi_{0\alpha}^\dagger(t) \vec{\sigma}_{\alpha\beta} \psi_{1\beta}(t) - \vec{S} \psi_{1\alpha}^\dagger(t) \vec{\sigma}_{\alpha\beta} \psi_{0\beta}(t) \right]. \quad (\text{A4})$$

The expectation value of the charge on the dot is then to second order in the coupling to the impurity

$$\begin{aligned} \langle \hat{Q} \rangle_2 &= e \frac{(\tilde{J}_{10})^2}{4} \sum_{a,b} \sum_{\alpha\beta} \int_{-\infty}^0 dt_1 \int_{-\infty}^0 dt_2 \langle S^a(t_1) S^b(t_2) \sigma^a \sigma^b \rangle \left[\langle \psi_{0\alpha}^\dagger(t_2) \psi_{0\alpha}(t_1) \rangle \langle \psi_{1\alpha}(t_2) \psi_{1\alpha}^\dagger(t_1) \rangle \right. \\ &\quad \left. - \langle \psi_{0\beta}(t_2) \psi_{0\beta}^\dagger(t_1) \rangle \langle \psi_{1\beta}^\dagger(t_2) \psi_{1\beta}(t_1) \rangle \right] \\ &= e \frac{3(\tilde{J}_{10})^2}{8} \int_{-\infty}^0 dt_1 \int_{-\infty}^0 dt_2 \left[\langle \psi_0^\dagger(t_2) \psi_0(t_1) \rangle \langle \psi_1(t_2) \psi_1^\dagger(t_1) \rangle - \langle \psi_0(t_2) \psi_0^\dagger(t_1) \rangle \langle \psi_1^\dagger(t_2) \psi_1(t_1) \rangle \right] \end{aligned} \quad (\text{A5})$$

where the averages are taken over the ground state of the uncoupled system. It is advantageous to Fourier transform the problem as:

$$\langle \hat{Q} \rangle_2 = -e \frac{3(\tilde{J}_{10})^2}{8} \sum_{p,k} \int_{-\infty}^0 dt_1 \int_{-\infty}^0 dt_2 \left[\langle a_k(t_2) a_k^\dagger(t_1) \rangle \langle a_p^\dagger(t_2) a_p(t_1) \rangle - \langle a_p(t_2) a_p^\dagger(t_1) \rangle \langle a_k^\dagger(t_2) a_k(t_1) \rangle \right] \quad (\text{A6})$$

where the momentum indices p and k respectively refer to the grain and to the reservoir. Using the Green's functions of the isolated grain:

$$\begin{aligned}\langle a_p^\dagger(t_2)a_p(t_1) \rangle &= \Theta(-\epsilon_p)e^{i(\epsilon_p-U_{-1})(t_2-t_1)} \\ \langle a_p(t_2)a_p^\dagger(t_1) \rangle &= \Theta(\epsilon_p)e^{-i(\epsilon_p+U_1)(t_2-t_1)},\end{aligned}\quad (\text{A7})$$

where again U_1 and U_{-1} embody the energies to add an electron and hole onto the grain, we finally find:

$$\begin{aligned}\langle \hat{Q} \rangle_2 &= -e \frac{3(\tilde{J}_{10})^2}{8} \sum_{k,p} \left[\frac{\Theta(\epsilon_k)\Theta(-\epsilon_p)}{(\epsilon_k - \epsilon_p + U_{-1})^2} - \frac{\Theta(-\epsilon_k)\Theta(\epsilon_p)}{(\epsilon_p - \epsilon_k + U_1)^2} \right] \\ &= e \frac{3(\tilde{J}_{10})^2}{8} \ln \left(\frac{e/2C - \varphi}{e/2C + \varphi} \right).\end{aligned}\quad (\text{A8})$$

Θ is the usual Heavyside function. Density of states in the grain and in the lead have been assumed to be equal and taken to be 1 for simplicity.

Now, we briefly want to show that cubic orders involve logarithmic divergences both associated with the Kondo coupling and with the proximity of a degeneracy point in the charge sector. More precisely, let us focus on the specific contribution in $J_0\tilde{J}_{10}^2$ for the term $\langle \hat{Q} \rangle_3 = \langle 0|\hat{Q}^{(1)}|2\rangle$, with

$$\begin{aligned}|2\rangle &= -\frac{1}{2} \int_{-\infty}^0 dt_1 \int_{-\infty}^0 dt_2 T[H_K(t_1)H_K(t_2)]|0\rangle \\ &= -\frac{J_0\tilde{J}_{10}}{2} \sum_{a,b} \sum_{\alpha\beta} \sum_{\mu,\nu} \int_{-\infty}^0 dt_1 \int_{-\infty}^0 dt_2 T[S^a(t_1)S^b(t_2)]T[\psi_{0\alpha}^\dagger(t_1)\frac{\sigma_{\alpha\beta}^a}{2}\psi_{0\beta}(t_1)\psi_{0\mu}^\dagger(t_2)\frac{\sigma_{\mu\nu}^b}{2}\psi_{1\nu}(t_2)]|0\rangle \\ &= -\frac{J_0\tilde{J}_{10}}{2} \sum_{a,b} \sum_{\alpha\beta} \sum_{\mu,\nu} \int_{-\infty}^0 dt_1 \int_{-\infty}^0 dt_2 T[S^a(t_1)S^b(t_2)]T[\langle\psi_{0\alpha}^\dagger(t_1)\psi_{0\nu}(t_2)\rangle\delta_{\alpha\nu}\psi_{0\beta}(t_1)\psi_{1\mu}^\dagger(t_2)\frac{\sigma_{\mu\nu}^b}{2}\frac{\sigma_{\nu\beta}^a}{2}]|0\rangle \\ &= +\frac{J_0\tilde{J}_{10}}{2} \sum_c \sum_\alpha \sum_{\mu,\beta} \int_{-\infty}^0 dt_1 \int_{-\infty}^0 dt_2 S^c \text{sgn}(t_1 - t_2) T[\langle\psi_{0\alpha}^\dagger(t_1)\psi_{0\alpha}(t_2)\rangle\psi_{1\mu}^\dagger(t_2)\frac{\sigma_{\mu\beta}^c}{2}\psi_{0\beta}(t_1)|0\rangle \\ &\approx -iJ_0\tilde{J}_{10} \sum_c \sum_{\mu,\beta} \ln\left(\frac{D}{k_B T}\right) \int dt_1 S^c \psi_{1\mu}^\dagger(t_1)\frac{\sigma_{\mu\beta}^c}{2}\psi_{0\beta}(t_1)|0\rangle.\end{aligned}\quad (\text{A9})$$

It becomes then obvious that $|2\rangle$ is (almost) proportional to $|1\rangle$; It is straightforward to show that this induces a third-order correction for the charge on the grain

$$\langle \hat{Q}(T) \rangle_3 \propto J_0(\tilde{J}_{10})^2 \ln\left(\frac{D}{T}\right) \ln\left(\frac{e/2C - \varphi}{e/2C + \varphi}\right).\quad (\text{A10})$$

Note that the appearance of the extra $\ln(D/T)$ factor clearly stems from the prominent renormalization of the lead-dot spin Kondo coupling J_0 on a charge plateau.

¹ D. P. DiVincenzo *et al.*, *Quantum Mesoscopic Phenomena and Mesoscopic Devices in Microelectronics*, eds I. O. Kulik and R. Ellialtuglu (NATO ASI, Turkey, June 13-25, 1999); cond-mat/99112445.

² For a short review see L. Kouwenhoven and L. Glazman, *Phys. World* **14**, 33, (2001).

³ D. Goldhaber-Gordon, H. Shtrikman, D. Mahalu, D. Abusch-Magder, U. Meirav, M. A. Kastner, *Nature*, **391**, 156, (1998); D. Goldhaber-Gordon, J. Göres, M. A. Kastner, H. Shtrikman, D. Mahalu, and U. Meirav, *Phys. Rev. Lett.* **81**, 5225 (1998).

⁴ S. M. Cronenwett, T. H. Oosterkamp, and L. P. Kouwenhoven, *Science*, **281**, 540, (2001).

⁵ W. G. van der Wiel, S. De Franceschi, T. Fujisawa, J. M. Elzerman, S. Tarucha, and L. P. Kouwenhoven, *Science* **289**, 2105 (2000).

⁶ H. C. Manoharan, C. P. Lutz, and D. M. Eigler, *Nature*, **403**, 521-515 (2000).

⁷ V. Madhavan, W. Chen, T. Jamneala, and M. F. Crommie, *Phys. Rev. B* **64**, 165412 (2001); V. Madhavan, W. Chen,

- T. Jamneala, M. F. Crommie, and N. S. Wingreen, *Science*, **280**, 567 (1998).
- ⁸ For a review, I. L. Aleiner, P. W. Brouwer, and L. I. Glazman, *cond-mat/0103008* (2001).
- ⁹ K. A. Matveev, *Zh. Eksp. Teor. Fiz.* **98**, 1598 (1990) [*Sov. Phys. JETP* **72**, 892, (1991)]; K. A. Matveev, *Phys. Rev. B* **51**, 1743 (1995).
- ¹⁰ H. Grabert, *Phys. Rev. B* **50** 17364 (1994); G. Göppert, H. Grabert, N. V. Prokof'ev and B. S. Svistunov, *Phys. Rev. Lett.* **81**, 2324 (1998).
- ¹¹ C. P. Herrero, G. Schön, and A. D. Zaikin, *Phys. Rev. B* **59**, 5728-5737 (1999).
- ¹² E. Lebanon, A. Schiller, and F. B. Anders, *cond-mat/0211656* (2002).
- ¹³ *Single Charge Tunneling*, edited by H. Grabert and M. H. Devoret (Plenum Press, New York, 1992).
- ¹⁴ For a review, see D. L. Cox and A. Zawadowski, *Adv. Phys.* **47**, 599 (1998).
- ¹⁵ Ph. Nozières and A. Blandin, *J. Physique* **41**, 193, (1980).
- ¹⁶ V. J. Emery and S. Kivelson, *Phys. Rev. B* **46**, 10 812 (1992); D. G. Clarke, T. Giamarchi, and B. I. Shraiman, *ibid.* **48**, 7070 (1993); A. M. Sengupta and A. Georges, *ibid.* **49**, 10 020 (1994).
- ¹⁷ K. Le Hur and G. Seelig, *Phys. Rev. B* **65**, 165338 (2002).
- ¹⁸ L. I. Glazman, F. W. J. Hekking, and A. I. Larkin, *Phys. Rev. Lett.* **83**, 1830 (1999).
- ¹⁹ Using a (Radio-Frequency) Single Electron Transistor, the charge can now be measured with an accuracy up to a thousandth of an electron; K. Lehnert (private communication).
- ²⁰ D. Berman *et al.*, *Phys. Rev. Lett.* **82**, 161 (1999); D. S. Duncan *et al.*, *Applied Phys. Lett.* **74**, 1045 (1999).
- ²¹ G. Zaránd, G. T. Zimányi, and F. Wilhelm, *Phys. Rev. B* **62**, 8137 (2000).
- ²² E. Lebanon, A. Schiller, and F. B. Anders, *cond-mat/0303248*.
- ²³ K. Le Hur and P. Simon, *Phys. Rev. B* **67**, R201308 (2003).
- ²⁴ T. Gramspacher and K. A. Matveev, *Phys. Rev. Lett.* **85**, 4582 (2000).
- ²⁵ Yu. V. Nazarov, *Phys. Rev. Lett.* **82**, 1245 (1999).
- ²⁶ L. Borda, G. Zaránd, W. Hofstetter, B. I. Halperin, and J. von Delft, *Phys. Rev. Lett.* **90**, 026602 (2003).
- ²⁷ T. Pohjola, H. Schoeller, and G. Schön, *Europhys. Lett.* **55**, 241 (2001).
- ²⁸ U. Wilhelm and J. Weis, *Physica E* **6**, 668 (2000); unpublished.
- ²⁹ D. Cox, *Phys. Rev. Lett.* **59**, 1247 (1987).
- ³⁰ C. J. Bolech and N. Andrei, *Phys. Rev. Lett.* **88**, 237206 (2002).
- ³¹ M. Fabrizio, A. F. Ho, L. De Leo, and G. E. Santoro, *cond-mat/0305328*.
- ³² J. R. Schrieffer and P. A. Wolff, *Phys. Rev.* **149**, 491 (1966).
- ³³ A. Hewson, *The Kondo Problem to Heavy Fermions*, Cambridge University Press, 1993.
- ³⁴ L. I. Glazman and M. E. Raikh, *JETP Lett.* **47**, 452 (1988); T. K. Ng and P. A. Lee, *Phys. Rev. Lett.* **61**, 1768 (1988).
- ³⁵ Y. Oreg and D. Goldhaber-Gordon, *Phys. Rev. Lett.* **90**, 136602 (2003).
- ³⁶ G. Zaránd, *Phys. Rev. B* **52**, 13459 (1995).
- ³⁷ I. Affleck, A. W. W. Ludwig, and B. Jones, *Phys. Rev. B* **52**, 9528 (1995).
- ³⁸ Y. Q. Li, M. Ma, D. N. Shi, and F. C. Zhang, *Phys. Rev. Lett.* **81**, 3527 (1998).
- ³⁹ P. Azaria, E. Boulat, and Ph. Lecheminant, *Phys. Rev. B* **61**, 12112 (2000); M. van den Bossche, P. Azaria, Ph. Lecheminant, and F. Mila *Phys. Rev. Lett.* **86**, 4124 (2001).
- ⁴⁰ N. E. Bickers, *Rev. Mod. Phys.* **59**, 845 (1987).
- ⁴¹ O. Parcollet, A. Georges, G. Kotliar, and A. Sengupta *Phys. Rev. B* **58**, 3794 (1998); A. Jerez, N. Andrei, and G. Zaránd *Phys. Rev. B* **58**, 3814 (1998).
- ⁴² K.G. Wilson, *Rev. Mod. Phys.* **47**, 773 (1975); T. Costi, in *Density Matrix Renormalization*, edited by I. Peschel *et al.* (Springer 1999).
- ⁴³ B. Jones and C. M. Varma, *Phys. Rev. Lett.* **58**, 843 (1987); B. Jones *et al.*, *ibid.* **61**, 125 (1988); B. Jones and C. M. Varma, *Phys. Rev. B* **40**, 324 (1989).
- ⁴⁴ Karyn Le Hur, *Phys. Rev. B* **67**, 125311 (2003).
- ⁴⁵ D. C. Ralph and R. A. Burhman, *Phys. Rev. Lett.* **69**, 2118 (1992); D. C. Ralph, A. W. W. Ludwig, J. von Delft, and R. A. Burhman, *ibid.* **72**, 1064 (1994); D. C. Ralph and R. A. Burhman, *Phys. Rev. B* **51**, 3554 (1995).
- ⁴⁶ A. Rosch, J. Kroha, and P. Wölfle, *Phys. Rev. Lett.* **87**, 156802 (2001).
- ⁴⁷ E. H. Kim, *cond-mat/0106575*, (unpublished).